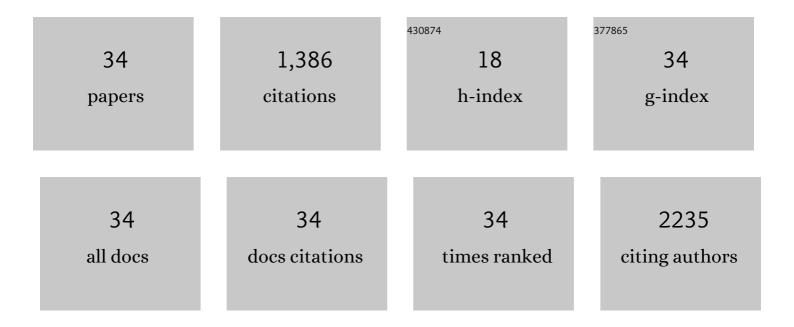
## Yaguang Li

List of Publications by Year in descending order

Source: https://exaly.com/author-pdf/2020835/publications.pdf Version: 2024-02-01



#	Article	IF	CITATIONS
1	Coke and sintering resistant nickel atomically doped with ceria nanosheets for highly efficient solar driven hydrogen production from bioethanol. Green Chemistry, 2022, 24, 2044-2050.	9.0	14
2	General heterostructure strategy of photothermal materials for scalable solar-heating hydrogen production without the consumption of artificial energy. Nature Communications, 2022, 13, 776.	12.8	56
3	Light-Irradiated Thermal Energy-Promoted Selective Phenol Hydrogenation on Cellulose-Supported Palladium Catalyst with Green Hydrogen. ACS Sustainable Chemistry and Engineering, 2022, 10, 9205-9215.	6.7	6
4	Weak sunlight-driven mass toluene combustion through scalable Cu doped CeO2 microspheres. Journal of Cleaner Production, 2021, 293, 125328.	9.3	4
5	Sewage-free preparation of 2D metal oxides by a rapid freezing soft template method for extraordinarily activating solar-driven humidity VOC combustion. Catalysis Science and Technology, 2021, 11, 2456-2460.	4.1	6
6	Solar-heating thermocatalytic H <sub>2</sub> production from formic acid by a MoS <sub>2</sub> -graphene-nickel foam composite. Green Chemistry, 2021, 23, 7630-7634.	9.0	7
7	Efficient hydrogen production <i>via</i> sunlight-driven thermal formic acid decomposition over a porous film of molybdenum carbide. Journal of Materials Chemistry A, 2021, 9, 22481-22488.	10.3	9
8	Ambient sunlight-driven photothermal methanol dehydrogenation for syngas production with 32.9 % solar-to-hydrogen conversion efficiency. IScience, 2021, 24, 102056.	4.1	12
9	A general bimetal-ion adsorption strategy to prepare nickel single atom catalysts anchored on graphene for efficient oxygen evolution reaction. Journal of Energy Chemistry, 2020, 43, 52-57.	12.9	85
10	Ni loaded on N-doped carbon encapsulated tungsten oxide nanowires as an alkaline-stable electrocatalyst for water reduction. Sustainable Energy and Fuels, 2020, 4, 788-796.	4.9	15
11	Efficient combustion of chlorinated volatile organic compounds driven by natural sunlight. Science of the Total Environment, 2020, 749, 141595.	8.0	14
12	Outdoor sunlight-driven scalable water-gas shift reaction through novel photothermal device-supported CuO <sub>x</sub> /ZnO/Al <sub>2</sub> O <sub>3</sub> nanosheets with a hydrogen generation rate of 192 mmol g <sup>â^'1</sup> h <sup>â^'1</sup> . Journal of Materials Chemistry A, 2020, 8, 19467-19472.	10.3	23
13	Triple Functions of Ni(OH) <sub>2</sub> on the Surface of WN Nanowires Remarkably Promoting Electrocatalytic Activity in Full Water Splitting. ACS Catalysis, 2020, 10, 13323-13333.	11.2	120
14	Realizing efficient natural sunlight-driven photothermal selective catalytic reduction of nitrogen oxides by AlNx assisted W doped Fe2O3 nanosheets. Solar Energy Materials and Solar Cells, 2020, 208, 110395.	6.2	10
15	Mass production of superhydrophilic sponges for efficient and stable solar-driven highly corrosive water evaporation. Environmental Science: Water Research and Technology, 2019, 5, 2041-2047.	2.4	5
16	Selective light absorber-assisted single nickel atom catalysts for ambient sunlight-driven CO2 methanation. Nature Communications, 2019, 10, 2359.	12.8	185
17	Fe3Si assisted Co3O4 nanorods: A case study of photothermal catalytic CO oxidation under ambient solar irradiation. Nano Energy, 2019, 62, 653-659.	16.0	36
18	Microwave Reaction: A Facile Economic and Green Method to Synthesize Oxygenâ€Decorated Graphene from Carbon Cloth for Oxygen Electrocatalysis. ChemCatChem, 2018, 10, 2305-2310.	3.7	7

YAGUANG LI

#	Article	IF	CITATIONS
19	Synthesis of mesoporous Fe <sub>3</sub> Si aerogel as a photo-thermal material for highly efficient and stable corrosive-water evaporation. Journal of Materials Chemistry A, 2018, 6, 23263-23269.	10.3	23
20	Synthesizing new types of ultrathin 2D metal oxide nanosheets via half-successive ion layer adsorption and reaction. 2D Materials, 2017, 4, 025031.	4.4	18
21	The crystalline/amorphous contact in Cu <sub>2</sub> O/Ta <sub>2</sub> O <sub>5</sub> heterostructures: increasing its sunlight-driven overall water splitting efficiency. Journal of Materials Chemistry A, 2017, 5, 2732-2738.	10.3	41
22	Passivation of defect states in anatase TiO2 hollow spheres with Mg doping: Realizing efficient photocatalytic overall water splitting. Applied Catalysis B: Environmental, 2017, 202, 127-133.	20.2	117
23	Fabrication of Fe <sub>2</sub> TiO <sub>5</sub> /TiO <sub>2</sub> nanoheterostructures with enhanced visible-light photocatalytic activity. RSC Advances, 2016, 6, 45343-45348.	3.6	38
24	Interfacial effect on Mn-doped TiO <sub>2</sub> nanoparticles: from paramagnetism to ferromagnetism. RSC Advances, 2016, 6, 57403-57408.	3.6	18
25	Synthesis of Na-doped ZnO hollow spheres with improved photocatalytic activity for hydrogen production. Dalton Transactions, 2016, 45, 11145-11149.	3.3	24
26	Synthesis of ZrO <sub>2</sub> :Fe nanostructures with visible-light driven H <sub>2</sub> evolution activity. Journal of Materials Chemistry A, 2015, 3, 2701-2706.	10.3	33
27	Preparation of ZnFe <sub>2</sub> O <sub>4</sub> nanostructures and highly efficient visible-light-driven hydrogen generation with the assistance of nanoheterostructures. Journal of Materials Chemistry A, 2015, 3, 8353-8360.	10.3	135
28	Enhancing photocatalytic activity for visible-light-driven H2 generation with the surface reconstructed LaTiO2N nanostructures. Nano Energy, 2015, 12, 775-784.	16.0	62
29	Epitaxial growth and thermoelectric properties of c-axis oriented Bi <sub>1â^'x</sub> Pb <sub>x</sub> CuSeO single crystalline thin films. CrystEngComm, 2015, 17, 8697-8702.	2.6	18
30	A Full Compositional Range for a (Ga <sub>1-<i>x</i></sub> Zn <i><sub>x</sub></i> )(N <sub>1-<i>x</i></sub> O <i><sub>x</sub></i> ) Nanostructure: High Efficiency for Overall Water Splitting and Optical Properties. Small, 2015, 11, 871-876.	10.0	77
31	A new type of hybrid nanostructure: complete photo-generated carrier separation and ultrahigh photocatalytic activity. Journal of Materials Chemistry A, 2014, 2, 14245-14250.	10.3	36
32	A new type of p-type NiO/n-type ZnO nano-heterojunctions with enhanced photocatalytic activity. RSC Advances, 2014, 4, 34649.	3.6	30
33	A facile fluorine-mediated hydrothermal route to controlled synthesis of rhombus-shaped Co3O4 nanorod arrays and their application in gas sensing. Journal of Materials Chemistry A, 2013, 1, 7511.	10.3	91
34	lodineâ€ionâ€induced Sizeâ€ŧunable Co <sub>3</sub> O <sub>4</sub> Nanowires and the Sizeâ€dependent Catalytic Performance for CO Oxidation. ChemCatChem, 2013, 5, 3576-3581.	3.7	11